14

Low-Wavelengths SOI CMOS Photosensors for Biological Applications

Olivier Bulteel, Nancy Van Overstraeten-Schlögel, Aryan Afzalian, Pascal Dupuis, Sabine Jeumont, Leonid Irenge, Jérôme Ambroise, Benoît Macq, Jean-Luc Gala and Denis Flandre
Université catholique de Louvain
Belgium

1. Introduction

Biological agents may be characterized (in terms of quantity (or concentration), purity, nature) using optical ways like spectrometry, fluorometry and real-time PCR for example. Most of these techniques are based on absorbance or fluorescence. Indeed, many biological molecules can absorb the light when excited at wavelengths close to blue and ultraviolet (UV). For example, DNA, RNA and proteins feature an absorption peak in the deep UV, more precisely around 260 and 280 nm (Karczemska & Sokolowska, 2001). This work is widely focused on those wavelengths. A biological sample concentration measurement method can be based on UV light absorbance or transmittance, as already known and realized with high-cost and large-size biomedical apparatus. But, often, the difficulties come from the limitation for measuring very small concentrations (close to a few ng$/\mu$L or lower) since the measurement of such small light intensity variations at those low wavelengths requires a precise light source, and very efficient photodetectors. Reducing the dimensions of such a characterization system further requires a small light source, a miniaturized photosensor and a processing system with high precision to reduce the measurement variations. Some light-emitting diodes (LED) performing at those UV wavelengths have recently appeared and may be used to implement the light source. Concerning the optical sensor, while accurate but high-cost photosensors in technologies such as AlGaN and SiC provide high sensitivies in UV low wavelengths thanks to their semiconductor bandgap (Yotter & Wilson, 2003), the silicon-on-insulator (SOI) layers absorb the photons in that specific range thanks to an appropriate thickness of the silicon. Adding excellent performances of low power consumption, good temperature behavior and high speed (Flandre et al., 1999; 2001), the SOI technology allows the designers for integrating a specific signal processing integrated CMOS circuit to transform the photocurrent into a digital signal for example. This opens the possibility to build a low-cost, complete and portable microsystem, including the light source, the photodetector and a recipient for the sample to characterize.

For this chapter, we start with a state-of-the-art describing the current DNA quantification methods with their advantages and disadvantages. Since we will work at low optical wavelengths, we review different ultraviolet light sources that are used in laboratories or in biomedical fields. A description of different photodetectors in various technologies, more especially in SOI, suitable for DNA quantification will then be presented. Afterwards, we

detail, the SOI photodiode and the integrated circuit that were used in our experiments for characterizing DNA concentration as well as the other particular biological agents. Finally, the results of our measurements are presented and discussed.

2. Current optic-based DNA quantification methods

Nowadays the DNA concentration in liquid samples may be measured by different techniques. For example, it is possible to quantify DNA by its property to absorb light around 260 nm. However, the DNA quantities are usually too small to be detected, so the DNA concentration has to be amplified. A very-well know method to amplify DNA is the polymerase chain reaction (PCR).

2.1 PCR related methods

The polymerase chain reaction consists in a cyclic repetition of different temperature stages of a solution containing the DNA to amplify, dNTPS, primer and the DNA polymerase enzyme. A heating stage is necessary to separate the two strands of the DNA. At the lower temperature, each strand is used as a template for the synthesis by the DNA polymerase. After a consistent number of cycles, the target DNA (determined by the primer) is amplified by a factor 2^x (where x is the cycle number). The DNA concentration can next be measured by two different ways :

– the agarose gel electrophoresis. This consists in a migration of the DNA in an agarose gel under a bias voltage. The size of the double stranded DNA is revealed by a luminescent incorporation agent and estimated by comparison with a DNA ladder used as reference. The detection is visual which is inconvenient because of its dependence on the personal visual accuracy.

– the quantitative real-time PCR. This method allows the measurement of DNA concentrations during the amplification of the DNA by the addition of aspecific fluorophores. Basically, one fluorophore is initially added to the solution and engraft to the double stranded DNA along with the increase of the DNA. After each cycle, the DNA solution is illuminated and the fluorophores grafted to the DNA are emitting a light at a specific wavelength. The emitted fluorescence is thus proportional to the DNA quantity. The main problem of the real-time PCR is the relatively poor efficiency of the fluorophores and thus the light emission does not always reflect the accurate DNA concentration.

Anyway, the PCR-based methods feature the disadvantages of a long measurement time before obtaining the results. Moreover, it requires a large-sized laboratory equipment, including a specific software for analyzing the results. They also depend on the PCR amplification efficiency which is not constant with the number of cycles and thus introduce a high variance on statistical analyses.

2.2 Spectrometry

Spectrophotometers are used in molecular biology to quantify DNA and also to assess its purity. The spectrometers use a method combining optic fiber and liquid tension to illuminate a droplet of a DNA sample with a UV light. The instrument measures the DNA absorbance at 260 nm and can also perform a measurement at 280 nm to detect the presence of contaminating proteins in the sample. The spectrometers allow for quick measurement but with a poor reproducibility.

2.3 Fluorometry

Fluorescence spectroscopy is used in biological quantification techniques. It requires fluorescent dyes that can specifically bind to the DNA or RNA molecules. The fluorometry is based on a measurement $90°$ of a fluorescent light emitted by a dye excited by the instrument. The fluorometry features a very statistically significant (i.e. inducing a very low variance) result but implies several manipulations, and a long analysis time.

3. The UV light sources

In order to fully take advantage of the UV absorbance property of the DNA, the samples must be illuminated with a light source at appropriate wavelength and power. In laboratories, the equipments described in the previous section feature light sources that are encumbering or expensive. Hereunder is a non-extensive list of such sources :

– the large spectrum lamp. That kind of lamp is mostly used for research. For example, halogen-deuterium lamps provide a spectrum from 200 nm to 1200 nm with large emitting power. Associated with a monochromator, they allow for selecting with precision any wavelength and measurement of the spectral response of a photosensitive device. They can also be used to simulate any monochromatic light source, at present between 250 and 400 nm. But often, the whole system (including the lamp and the monochromator) is too voluminous to be integrated in a portable device.

– the flash lamp. In the spectrometers, Xenon flash lamps are used. They feature an emitting spectrum for which the high emission peak is around 260 nm. This kind of lamp provides a high power but unfortunately generates second order peaks at higher wavelengths so that a precise photosensor is required to detect only the transmitted light at 260 nm or precise filters must be integrated to cut off the parasitic wavelengths. This could lead to a sensible loss of light power.

– the laser. In the PCR apparatus for example, the light source used to excite the fluorophores has to be very powerful and narrow around the exciting wavelength. The best choice is thus a laser. But apart from these excellent optical characteristics, a laser is very expensive and not suitable for a portable application, since it requires a stabilized supply power and is not miniaturizable.

– the fluorophores. These chemical components allow the detection of a molecule. They are used in the PCR to visually follow the amplification of a target DNA during the exponential stages of the PCR. The nature of the fluorophores may be various. For example, SYBR Green fluorescent dyes bind to the double stranded DNA molecules and emit after excitation a light at a specific wavelength when the DNA is re-assembled. So the emission depends on the hybridization rate of the DNA. Another example is the Taqman probe which, contrarily to the SYBR Green, is based on the FRET principle : a probe is covalently bonded with a fluorophore and a quencher inhibits its fluorescence. Once the exonuclease activity of the polymerase degrades the probe, fluorescence is generated by the fluorochrome. But even if the nature of the fluorophore may be quite different, their common characteristic is their dependence on their affinity with their target and a relatively poor emission requiring so a long observation time (in order to integrate a sufficient photocurrent) and a very low-noise photosensor.

– the light emitting diode (LED). Finally, to combine the advantages of a high emitting light power, a controlled and narrow emitting spectrum, and a low fabrication cost, the LEDs

are an opportunistic choice. To ensure a low wavelength emission spectrum, the materials used to fabricate a UV diode are diamond (C), and Al-based materials (i.e. AlN and AlGaN) thanks to to their large bandgap, allowing a high energy photons generation when the electron-hole pairs are recombining. The UV LEDs have to be biased with relatively high forward voltage (e.g. Vd=6 V) which yields a current of about Id$\simeq$20 mA. This implies a consistent power needed to bias the diodes (compared to the power needed to supply a microelectronic integrated circuit), which also has to be very stable in time to minimize the fluctuations of the emitted light and reduce the measurements errors. However LEDs are miniaturized, portable and low-cost UV light source, making them good candidates for a complete optoelectronic microsystem aiming at biomedical applications.

4. The optical sensors for biomedical applications

In the previous laboratory equipments, optical sensors are used to measure a fluorescence phenomenon or a transmitted/absorbed light. In those equipments, the sensors are often charge coupled devices (CCD), eventually associated with a mirror network in order to select the appropriate wavelength to measure. CCDs feature the advantage of good linearity, and signal to noise ratio. But they also require a complex embedded electronic circuit to generate the clocks needed to control the charges transfers. In our case, since we target a portable, low-cost and easy-to-use system, a single device photosensor will be considered.

The most common used optical sensor to detect a signal is a photodiode. As we extensively study the UV and blue sensitive photosensors, we present a short state-of-the-art of the main available devices in each technology. A wide review of such photosensors has also been reported by Yotter & Wilson (2003). An important figure of merit for an optoelectronic sensor is the responsivity (R) :

$$R = \frac{I_{ph}}{P_{in}}[A/W] \tag{1}$$

defined as the ratio between the light induced current I_{ph}, called the photocurrent, and the incident light power at the diode surface Pin. Some papers also refer to the external quantum efficiency (QE) of the device defined as :

$$QE = \frac{\frac{I_{ph}}{q}}{\frac{P_{in}}{h\nu}}[\%] \tag{2}$$

where h is the Planck's constant and ν is the frequency related to the wavelength λ by $c = \nu \cdot \lambda$ where c is the vacuum speed of light.

Both are expressed as a function of the wavelength, so it is easy to compare devices for a given spectral range of detection, i.e, blue and UV in our case. More precisely, since DNA is absorbing at 260 nm and blue is defined from 450 to 475 nm in the electromagnetic spectrum, we can only compare the device on the specifications given in the papers. Three technology categories are studied below : bulk silicon, SOI and another regrouping some of the most common other used materials.

4.1 In bulk silicon technology

Silicon remains the lowest-cost material to fabricate a photodiode and can absorb photons whose correspond to a wavelength up to slightly more than 1100 nm thanks to its 1.1 eV bandgap (Zimmermann, 2000). Unfortunately, to realize a spectral filter, in order to only

absorb photons with an associate low wavelength, a low thickness of the silicon is needed since most of the photons are absorbed in the first 5 μm of the silicon thickness. This leads to reducing as much as possible the thickness of the silicon region where the photons are absorbed and to reduce the reflections. Consequently, a high responsivity can be achieved in the appropriate wavelength by other techniques like spatial modulation of light (Chen & du Plessis, 2006) or special devices such as avalanche diode (Pauchard et al., 2000).

4.2 In SOI technology

Silicon-on-insulator is a particular silicon-based technology in which a thin silicon film is separated from a thick silicon substrate with an oxide layer (called the buried oxide, or BOX). When fabricating an integrated circuit, the electronic devices (including transistors, capacitors, resistors, ...) are realized in the top thin layer. This insulated structure features the advantage to considerably reduce the leakage currents of the transistors, reduce the parasitic capacitances of the circuits, and improve the resistance of the circuitry to the variations of temperature (at low as well as high temperature, from 100 K to 450 K (Flandre et al., 1999; 2001)).

Silicon absorbs light as a function of its thickness: the thicker the silicon, the higher the absorbed wavelengths. So, contrarily to a classical photosensor embedded in a thick silicon wafer, which absorbs most of the light from UV to near infra-red, a SOI device featuring a thin film with 100 nm of thickness allows for only absorbing light whose wavelength is under 450 nm.

4.3 Other semiconductor materials

Silicon is the most common semiconductor but other materials can be used to implement a photosensor. Thanks to their larger bandgap, materials based on Gallium Nitride (GaN) can more easily absorb photons associated to low wavelengths independently from its thickness and then achieve high responsivities below 400 nm (Chang et al., 2008; 2006; Biyikli et al., 2005; Monroy et al., 2001). Other frequently used technology is the silicon carbide (SiC) that has proven its interest by the past (Brown et al., 1998; Fang et al., 1992).

4.4 Anti reflection coatings

The advantage of depositing a dual-layer anti-reflection coating (ARC) above a photodiode has been proven (Kumer et al., 2005). It can considerably reduce the reflections of light by an accurate choice of thickness according to the index of refraction of the material and the wavelength at which the efficiency has to be improved. The most common ARCs are silicon oxide (SiO_2), silicon nitride (Si_3N_4) and alumina (Al_2O_3). Great advances have been made in the solar cell laboratory research concerning ARC. Recently, the researches are more focused on the development of texturized surfaces which are also often used to ensure a greater absorption of the light in the device with multiple reflections at the incident interface. The patterned protective layers allow an augmentation of their transmittance, leading to an increase of the quantum efficiencies of the cells (Han et al., 2009; Chu et al., 2008; Gombert et al., 2000).

4.5 Summary and comparison

The table 1 summarizes most representative results for the previously cited technologies. For classical Si photodiodes (i.e. except for avalanche diodes or else), SOI technology remains much more efficient than classical bulk silicon as can be seen on the table above.

Source	Techno	Performance
Torres-Costa et al. (2007)	Bulk Si	R=0.025@400 nm
Chen & du Plessis (2006)	Bulk Si	R=0.05@400 nm
Pauchard et al. (2000)	Bulk Si (Avalanche)	R=0.17@400 nm
Bulteel et al. (2009)	SOI	R=0.1@400 nm
Afzalian & Flandre (2005)	SOI	R=0.015@430 nm
Miura et al. (2007)	SOI	NA
Chang et al. (2008)	GaN	R=0.15@[300-400] nm
Chang et al. (2006)	GaN	R=0.18@350 nm
Biyikli et al. (2005)	AlGaN	R=0.1@250 nm
Monroy et al. (2001)	AlGaN	R=0.2@350 nm
Brown et al. (1998)	SiC	R=0.15@280 nm
Fang et al. (1992)	SiC	R=0.26@380 nm
Han et al. (2009)	Si and Patterned ARC	QE=60@400 nm

Table 1. Comparison of the photodiode characteristics among the different technologies

Comparatively, the larger bandgap materials can achieve a higher responsivity, but their fabrication cost is much higher and even if SOI technology reaches a lesser responsivity, its value remains on the same order of magnitude as the other semiconductor materials.

5. The SOI photodiode design

As previously said, a very common electronic device, but with good efficiency, used to measure the light intensity is the diode, or the PN junction. By adding an intrinsic or low-doped region between the P and N regions, we obtain a PIN diode which can reach better optical response (Zimmermann, 2000). When realizing this device in the thin film of a SOI wafer, we implement a lateral PIN diode. This device has been used in this abstract as a reference, according to the good results found in the literature and its compatible fabrication with a standard CMOS process (Afzalian & Flandre, 2005). The photocurrent, previously introduced in equation 1, can also be defined as:

$$I_{ph} = I_D - I_{Dark} [A] \tag{3}$$

where I_D is the total current flowing through the diode and I_{Dark} is the dark current of the diode, i.e. the current through the diode when subject to no illumination. Referring to equation 1, the responsivity can thus be enhanced by increasing the photocurrent, which is can be obtained by reducing the dark current and optimizing the reverse bias of the photodiode, Vd. Raising Vd indeed increases the region where the photons generate electron-hole pairs (Afzalian & Flandre, 2005), however, the generation current also increases, but so does the dark current that itself decreases the photocurrent, and thus the responsivity. It has also been demonstrated that adding an anti-reflection coating greatly improves the sensitivity of the photodiode. In our case, a silicon nitride ARC has been deposited over a silicon dioxide that came naturally with the fabrication process. The cross section of a PIN diode in a SOI technology is shown in figure 1.

For the tested technology, the dimensions according to figure 1 were T_{SUB}=800 μm, T_{BOX}=400 nm, T_{Si}=80 nm, T_{OX}=280 nm and T_{ARC}=40 nm. For the diode itself, simulations have demonstrated that an intrinsic length of Li=8 μm could reach a maximum efficiency in our detection range while the anode and cathode lengths of Ln=Lp=10 μm are fixed by the
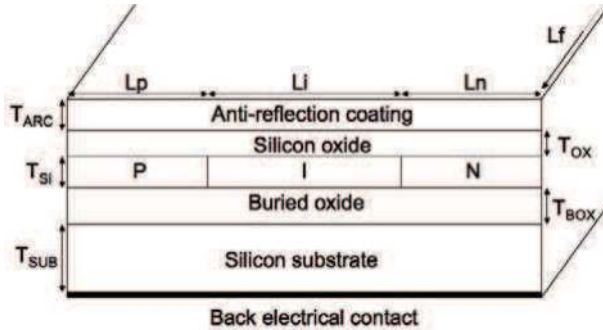
Fig. 1. Cross section of one finger of the SOI PIN photodiode

process (Flandre et al., 1999; 2001). A mathematical model has been implemented in Matlab for simulating the responsivity of our SOI device with a reflection-transmission of waves through a multi-layer device with thicknesses and refraction indexes as variables. But since the standard SOI wafer substrate and oxide are imposed by the fabrication process, while the thin Si film and the CMOS process oxide thicknesses are also constant on the wafer, the only left parametrical layer is the additional ARC. As demonstrated in (Kumer et al., 2005), we can minimize the reflected power by depositing two anti-reflecting coatings on top of a semiconductor layer. While the first ARC is the existing silicon oxide of 280 nm previously presented, the second top layer is most commonly a silicon nitride for its refraction index close to 2. Figure 2 presents the variation of responsivity at 400 nm as a function of the thickness of the silicon nitride top ARC. One can observe its periodicity as predicted in (Zimmermann, 2000; Kumer et al., 2005).

After fabrication, the photodiode responsivity has been measured by sweeping the electromagnetic spectrum in the range from 200 nm to 750 nm with a halogen-deuterium lamp and a monochromator selecting the appropriate wavelength. The comparison between the simulated and the measured responsivity is shown in figure 3.

One can observe high responsivities in the UV range while the responsivity falls down after 450 nm, which corresponds to the end of the blue range in the visible spectrum of
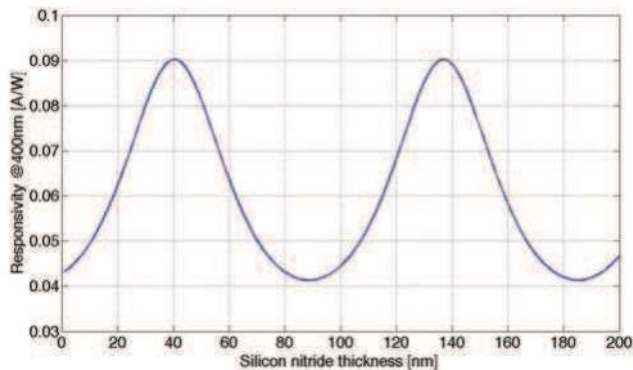

Fig. 2. Simulation of the responsivity at λ=400 nm of PIN photodiodes with a structure as in figure 1 as a function of the silicon nitride ARC.
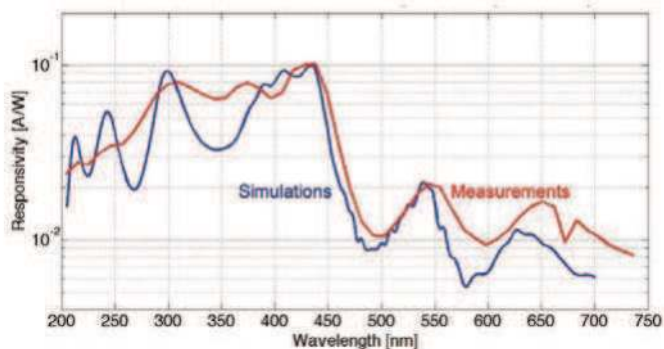
Fig. 3. Comparison between simulation and measurements of the photodiode responsivity

light. There is also a good correspondence between measurements and simulation, except for the attenuated experimental oscillations below 400 nm that can be explained by process non-uniformities. Based on the initial SOI wafer, other more accurate photodiodes can be designed according to the target light as in (Bulteel & Flandre, 2009), where it is proven that aluminum oxide ARC and silicon-on-nothing based structures may also be used to optimize such biological measurements.

6. The integrated circuit

6.1 Overview of the system

As previously mentioned, instead of directly measuring the current of the photodiode, a signal processing circuit can be fully integrated on a single chip with the photodiode, thanks to the same CMOS process and the SOI technology. An example of transimpedance circuit for measuring an analog voltage has been fully designed and measured in Afzalian & Flandre (2006). Another type of circuit can be used to transform the analog output of the photodiode into a digital signal, easy to interface with a microcontroller. An example of such a circuit is presented in figure 4.

This circuit corresponds to a current-to-frequency (I-f) converter. First, the photocurrent is processed by an integrator, and the integrated current has thus the shape of a rising voltage
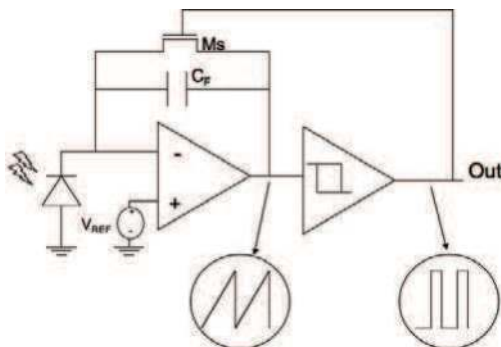

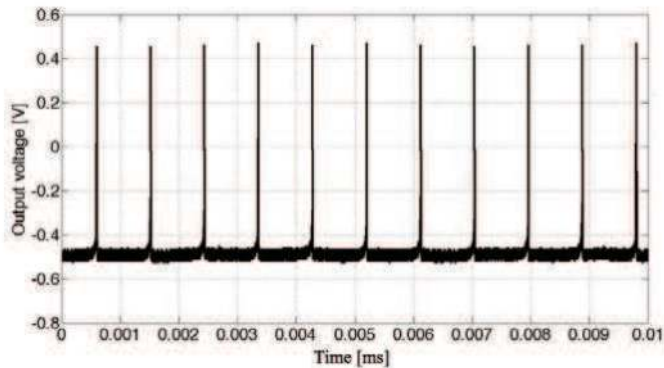Fig. 4. Schematic of the complete photodiode and signal processing circuit

Fig. 5. Output voltage of the current to frequency circuit

whose slope directly depends on the magnitude of the photocurrent flowing through the capacitor C_F. A two-thresholds comparator (implemented in this case by a Schmitt trigger) next transforms the integrated voltage into a squared signal that resets the integrator when the output becomes high. This simple system produces a number of pulses per second proportional to the amplitude of the photocurrent. So, for a fixed time of observation, the higher the photocurrent (i.e. the higher the UV intensity), the larger the number of pulses to be measured.

6.2 Design
The system can be tuned for the application to operate. For high current, and so high pulse frequencies to measure, the bandwidth of the operational amplifier may vary, as well as its open-loop gain depending on the precision required for the integrated function. For the measured photodiode, an implementation of this circuit was designed and fabricated in our SOI technology (Flandre et al., 1999; 2001) including a Miller operational amplifier with a 60 dB open-loop gain and a 3 MHz gain-bandwidth product (GBW). A 10 pF capacitance is used as a feedback to realize the integrator function while a SOI NMOS transistor with minimal dimension and a $\frac{W}{L} = 1$ ratio was chosen to reset the integrator ensuring minimal leakage current (Luque et al., 2003). With that choice, assuming that the output dynamic of the integrator (i.e. corresponding to the difference between the two thresholds of the following trigger) is set to 1V, a 10 pA photocurrent will charge the feedback capacitance within one second. Many types of Schmitt triggers (or other comparators) can be used, also depending on the required output and the switch. A similar circuit was found in the literature (Simpson et al., 2001; Bolton et al., 2002), but featuring a single threshold comparator. In our case, due to the very low luminous intensities to measure, the currents are very small and so is the slope of the integrated signal. We thus need a larger dynamic at the integrator output implying the use of a two thresholds comparator. A standard CMOS Schmitt trigger (Filanovsky & Baltes, 1994) was used for the comparator with an input dynamic of 1V as previously said.

The circuit is powered with a 2 V voltage and consumes approximately 600 μA. The whole chip including a 0.25 mm^2 photodiode, features an area of 0.5 mm^2. Its output under illumination is shown in figure 5.

One can observe the good behavior of the circuit. The circuit has also been illuminated with lights of different powers and wavelengths, and the experiment has proved the good
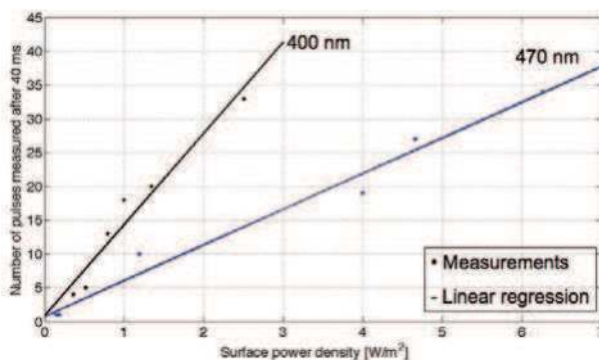
Fig. 6. Number of pulses measured in 40 ms as a function of the surface power density of light for 400 nm (black) and 470 nm (blue)

linearity of the outputs with regards to the responsivity of the photodiode (Bulteel et al., 2009) as showed in figure 6. One can observe that the slope ratios of the measurements linear regressions is of about 3 between 400nm and 470nm. When referring to the figure 3, the ratio of the responsivities at 400 nm and 470 nm is also of 3. As such, the integrated system can be used to measure environmental UV or DNA concentration.

7. Biological application of the SOI photodiodes

The current optical measurement methods (presented above in this chapter) require a lot of manipulations (e.g. pipetting, purification, etc.) and are not convenient for portable and low-cost applications. We present here an innovating system to measure DNA concentrations by optic transmittance. As previously introduced, the DNA features an absorption peak around 260 nm, so that its concentration in a liquid sample can be assessed by measuring a ray of light passing through the DNA solution. According to the Beer-Lambert law, the DNA concentration can be directly deduced from the light transmitted through the sample. Previous results demonstrated the feasibility of such a system (Bulteel et al., 2009) with a monochromator and our SOI photodiode based on measurements. The early results of the experiments were compared to spectrometry, fluorometry and quantitative real-time PCR. It was shown that the PCR featured the highest detection range but a poor precision and reproducibility. The spectrometry-based method has the lowest detection range and a poor precision. Fluorometry-based quantification presented the highest precision and a relatively good detection range, reaching the one obtained with the SOI photodiode.

7.1 The setup
Figure 7 shows a setup of the second experiment. Starting with a light source, implemented with a LED with appropriate wavelength, we can place the DNA in its container to be directly illuminated by the almost monochromatic light. Finally the sensor is positioned to receive the light that has passed through the DNA in order to measure the transmitted light.

7.2 Measurement of DNA samples in quartz containers
First of all, we wanted to confirm the literature reported results and compare them with those obtained with our system. Thus, we measured DNA samples from *Escherichia coli* in a
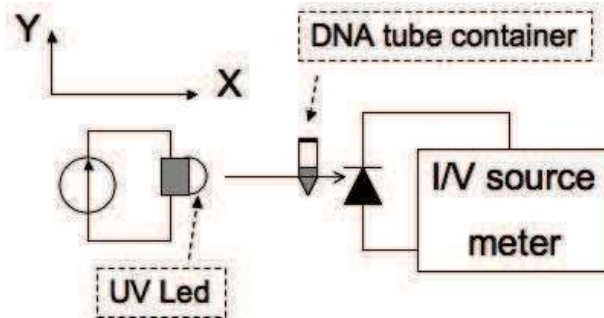
Fig. 7. Schematic of the system : a UV LED illuminates the DNA sample and the transmitted light is measured by a SOI photodiode coupled to a IV meter

reference absorption cell from Hellma. These cuvettes are 50 μL quartz containers whose good UV transmittance is a well-known property. The light is focused on a 2.5 mm diameter circular transparent window confining the DNA in a small cylinder illuminated by the light source. For the first step, the emitting wavelength of the LED was 260 nm. The LED was biased and monitored by a Keithley 236 IV source associated with a four wire connection ensuring a minimal noise floor needed for the small currents to measure (i.e. a few nA). Genomic DNA was pipetted and deposited in the quartz cuvettes with concentrations ranging from 400 ng/μL to 400 pg/μL. Three currents were measured for calibrating the system : the dark current of the photodiode, the photocurrent generated directly by the light source (denoted *Light*), and the photocurrent resulting of a blank measurement consisting of 50μL of water in the quartz cuvettes (denoted H_2O) as referred in figure 8 showing the photocurrents of the experiment. Under a Vd=-0.5 V reverse bias, a dark current average of 45 pA was measured. A monotonic relation between the photocurrent and the DNA concentration was observed. As previously demonstrated in Bulteel et al. (2009), the higher the DNA concentration, the more UV light is absorbed, and the lesser the induced photocurrent is generated in the diode. Evenly the lowest DNA concentration implied the highest photocurrent. This photocurrent
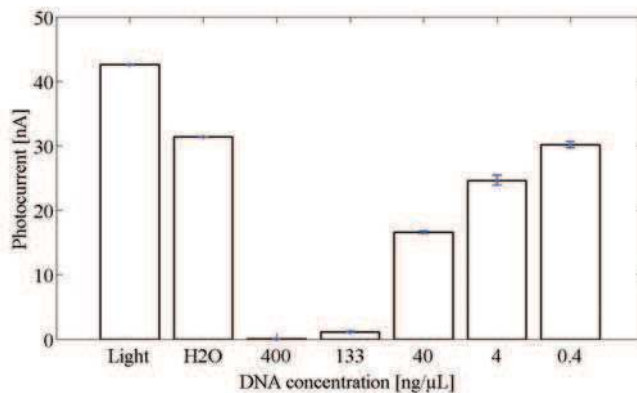

Fig. 8. Detection of different DNA concentrations (*Escherichia coli*) in the quartz cuvettes: Light and H_2O concentrations were used as references
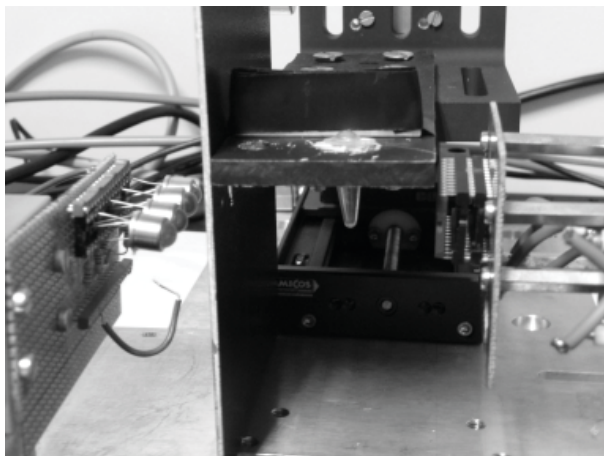
Fig. 9. Photograph of the tested system

was not significantly different from the blank sample. The error bars also shown in the figure correspond to the standard variations at each DNA concentration and pose another limit to the precision as discussed below.

8. Results of in-tube measurement with photodiode

The first step of our methodology demonstrated the principle of DNA measurements in a quartz container with a LED as light source and SOI diode as photosensor. But one condition to be fulfilled by the DNA container is to be as transparent as possible so that the light can interact with the DNA sample with as much optical power as possible. Therefore, we next practiced our experimentations on 200 μL PCR tubes, as they have already proven their usability (Bulteel et al., 2009). Another advantage is that while the quartz absorption cells require pipetting, drying and cleaning steps, the tube containers allow wasteless measurements with minimal manipulation steps and are much cheaper. A photograph of the setup is shown in figure 9.

On the left of the photograph, one can see a rack line of four LEDs emitting respectively at 260 nm, 280 nm, 295 nm and 360 nm. They are mounted on a XYZ displacer allowing for a selection of the most suitable wavelength according to the molecular nature of the biological target. The photodiode stands on the right of the picture and is encapsulated in a DIL-24 package (also mounted on a XYZ displacer for alignment) while the PCR tube is centered in the photograph on a two dimensional YZ displacer.

8.1 Detection limit and other statistical considerations

When dealing with biological samples in order to establish faithfully their concentration, it is crucial to compare the results to commonly used statistical definitions (Ripp, 1996). The most used functions are the precision limit (PL), the minimum detection limit (MDL) also called the limit of detection (LOD) for the laboratory measurements, and the limit of quantification (LOQ). Those are first linked to the blank sample measurements. So, for 20 measurements of a blank tube containing a solution without DNA (i.e. H_2O), the precision limit can be defined as :

$$PL = 3 \cdot \frac{\sigma_{Blank}}{\bar{X}_{Blank}} \tag{4}$$

Since the number of our measurements is less than 30 per sample, the results are distributed along a Student distribution, associated with its t-value. Secondly the MDL for a DNA concentration is defined with its t-value compared to the blank measurements as :

$$MDL = (t - value)_n \cdot \sigma_{Blank} = LOD \tag{5}$$

And finally, the LOQ is calculated as follow :

$$LOQ = 10 \cdot \sigma_{Blank} \tag{6}$$

The precision limit will be mainly discussed furtherly on this chapter.

8.2 Placement

The system is firstly calibrated with no assay tube. For a fixed position of the LED and the blocking mask, the photodiode is placed for obtaining a maximal value of the generated photocurrent under illumination. Then, a PCR tube containing an *europium*-diluted solution is hold on the YZ tube displacer and positioned to induce a minimal value of the photocurrent while fluorescence of the *europium* can confirm the correct alignment of the LED, the sample and the photodiode.

8.3 Description of the varying parameters

8.3.1 The light source

Since the LEDs are packaged with an hemispherical lens providing a straight illumination diagram, an aperture mask composed of a dark mask with a 2.5 mm diameter circular window is used to focus the light on the tube. The blocking mask is shown in figure 9 between the LEDs and the assay tube. The aperture mask also prevents from the diffraction of the light on the rounded boundaries of the PCR tube, which could perturb the measurements. Among the four available LEDs in the system previously presented, the two with emitting peak wavelengths of 260 nm and 280 nm were used, respectively for the DNA and proteins measurements. It is established that DNA absorbs the light at 260 nm while proteins are more sensitive to a 280 nm illumination, but both wavelengths were tested on each target, the ratios of the measurements enabling purity assessments. The LEDs have also been characterized with a spectrophotometer showing the inverse correlation between their illuminating power and the distance. Therefore a modulation of the optical power of the LED is possible when displacing it from the PCR tube.

8.3.2 The distance

As discussed above, the LED power illuminating the sample tube can be modulated by the distance between the LED and the tube. While the tubes are at 1 cm from the photodiode, and the blocking mask is also fixed (at a distance of 1.5 cm of the tube, i.e. 2.5 cm from the photodiode), the LEDs were disposed at three distances from the photodiode : 4.5 cm, 6.5 cm and 8 cm, which corresponds to a reduction of the power by respectively two and three whereas the closest distance displaying the highest power was 4.5 cm.

8.3.3 The photodiode bias

As discussed before, the choice of the photodiode bias is a trade-off between the dark and the photogenerated currents. Moreover, the measurement noise is highly related to the shot noise of the diode, defined as :

$$I_{Noise}^2 = 2 \cdot q \cdot I_D [A^2/Hz] \tag{7}$$

This implies a limit for the current to fill with the MDL of the system. In the experiments, a reverse voltage sweep range from 0 V to -5 V was applied to the diode and has lead to choose a reverse bias of Vd=-0.5V to maximize the photocurrent under a constant λ=280 nm illumination. It implies a dark current I_{Dark} of about 30 pA/mm^2 for the following experiment results. The optical dynamic (OD) is the value of the current of a blank sample reported to the dark current (Bulteel et al., 2009). When PCR tubes were used, the current measured with a blank sample was of 3 nA. We then calculated that the OD was of 100, while it was of 700 with the quartz cuvettes.

8.4 Results and discussion

To validate the system, two types of samples were tested and the results are reported in this section. Firstly, pure genomic DNA (*Escherichia coli*), and secondly, spores from bacteria (*Bacillus subtilis*). Each substance was diluted into the microtubes to a volume of 50 μL (corresponding to the same volume as in the quartz cuvettes) and each tube was measured four times with the LEDs emitting at λ=260 nm and λ=280 nm. The repeated measurements are essential to take into account the tube displacements, the heterogeneity of the solution (each tube is periodically vortexed to re-homogenize the solution) and other measurement fluctuations.As discussed for the quartz calibration experiment, since the lowest concentration provides the highest photocurrent, all results are displayed as a percentage of the maximal measured current. This enables a normalization of the different tests over the optical dynamic.

8.4.1 Measurement precision

The precision of our system, as introduced above in the statistical considerations section, was calculated to be 2.16 % over 20 blank measurements and multiplied by 3 to compute the precision limit (PL) from the maximum measured current, as can been seen in the curves of figures 10-12. The intersection of the precision limit and the sample curve yields an estimate of the lowest limit of detection range.

8.4.2 The DNA

The genomic DNA was extracted from *Escherichia coli*, a Gram negative bacterium, and diluted in concentrations ranging from 400 ng/μL to 4 pg/μL. Figures 10 and 11 report the data for the DNA concentrations that have been measured for the two wavelengths (260 and 280 nm), at the three LED-to-photodiode distances.

As expected, one can observe a monotonic relation between the photocurrent and the DNA concentration in both figures and shown by the calibration data of figure 8. Nevertheless, a closer analysis of the curves can point out the influence of the parameters.

– A first observation is that the LED emitting at λ=280 nm allows a detection range down to 4 pg/μL, which is better than the detection threshold of 40 pg/μL when the LED of λ=260 nm is at a distance of 4.5 cm. Concerning the other distances, the low detection range limits appear for 4 ng/μL and 40 pg/μL at 260nm and 280 nm respectively. This observation has already been made (Bulteel et al., 2009), and the phenomenon may be explained by the fact
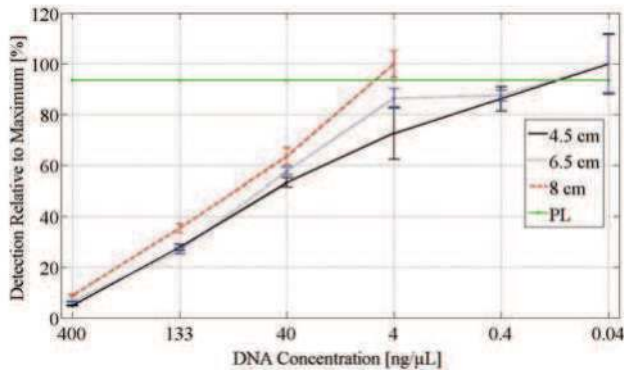
Fig. 10. Influence on the DNA concentration measurements of the distance between the LED at λ=260 nm and the photodiode : 4.5 cm (solid line), 6.5 cm (doted line), 8 cm (dashed line) and precision limit, PL (-x-)

that the peak absorption is too high at 260nm, implying a lower threshold for the detection. On the opposite, the slope of the absorption spectrum is lower at λ=280 nm (Karczemska & Sokolowska, 2001) and that would so enable more accurate measurements.

– About the LED emitting at λ=260 nm, when decreasing the power, the upper detectable concentration decreases. The upper limit of the detection seems to increase linearly with the distance. This makes sense since the measurement is made at the absorption peak wavelength. In opposition, the distance relation is less clear for λ=280 nm.

– It appears that the measurements realized at λ=280 nm are more precise with regards to standard deviation and are more reproducible than at λ=260 nm. The excessive absorption at 260 nm might disturb the level of detection, and this phenomenon may increase when if the power fits with the maximum absorption. Contrarily, the measurements carried out at 280 nm imply less variations on the results because of the lower but more reproducible
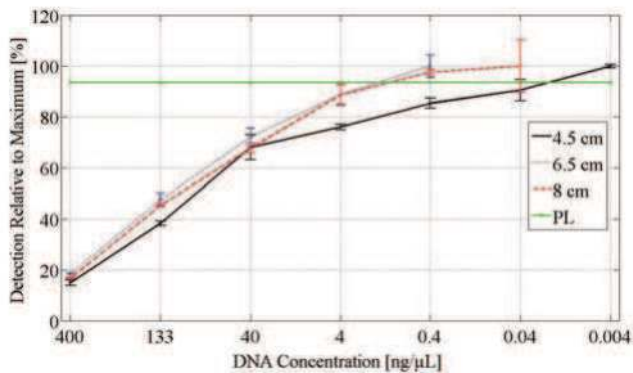

Fig. 11. Influence on the DNA concentration measurements of the distance between the LED at λ=280 nm and the photodiode : 4.5cm (solid line), 6.5cm (doted line), 8cm (dashed line) and precision limit, PL (-x-)
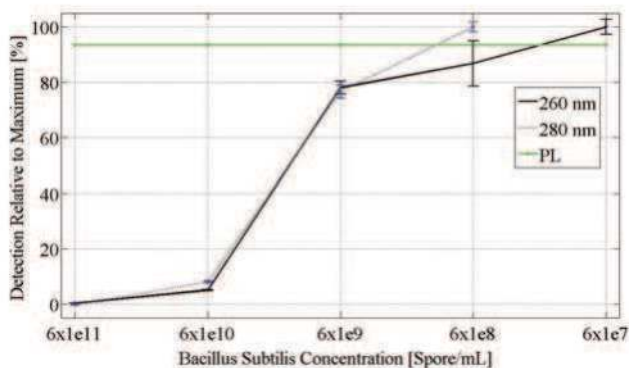
Fig. 12. *Bacillus subtilis* concentration measurements at 260 nm (solid line) and 280 nm (doted line) at a LED-to-photodiode distance of 6.5 cm. Precision limit is indicated as PL (-x-)

absorption of DNA around this wavelength.

– The standard deviation generally increases at both wavelengths, except for the shortest distance at 280 nm, with the diminution of the concentration under characterization. A usual trade-off between sensitivity and noise must hence be determined. In figure 11, the best threshold of detection then appears to be 0.02 ng/μL when the PL line crosses the measurement curve.

8.4.3 The bacteria

Lyophilized spores of a Gram positive bacterium (*Bacillus subtilis*), were resuspended in water in concentrations ranging from $6x10^{11}$ spores/mL to $6x10^{4}$ spores/mL. Figure 12 presents the in-tube measurements for both wavelengths. The measurements at λ=260 nm can cover a range down to $6x10^{7}$ spores/mL, and a decade lower for the LED at 280 nm. Nevertheless, the measurements at 280 nm are more precise in the measured range compared to those at 260 nm. Indeed the standard deviation at 260 nm for the concentration of $6x10^{8}$ spores/mL is larger.

9. Measurements with the integrated system

As previous experiments have demonstrated that DNA concentration can be measured with a UV SOI photodiode and a UV light source, this should also be possible with the complete integrated system presented in the section 6 of this chapter. The experiment has been made by replacing the photodiode chip with a current-to-frequency converter and its associated photodiode single chip. The 260 nm LED has been used to light the DNA tubes at a distance of 4.5 cm to the tubes. It was biased with a Keithley 2400 I-V source as well as the integrated circuit. The output pulse repetition periods were measured using an Agilent MSO8104A 1-GHz real-time oscilloscope. A dark measurement gave a result of three pulses only for a 50 seconds observation period. The precision limit has been measured over 20 blank tubes as for the photodiode experiments.

In a first experiment the same DNA concentrations as used previously (i.e. from 400 ng/μL to 4 pg/μL) are measured over a time period of 10 seconds. In figure 13, the number of pulses
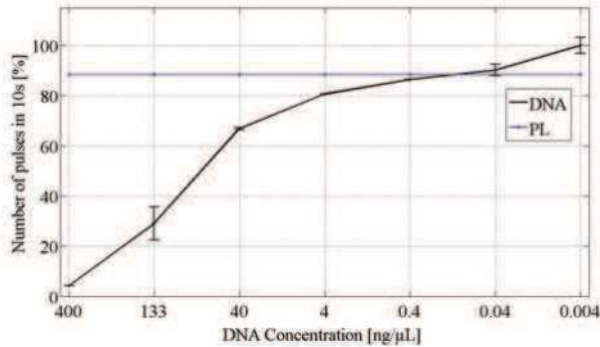
Fig. 13. DNA concentration measurement from 400 ng/μL to 4 pg/μL for 260 nm with the I-f circuit during a 10 seconds measurement period (solid line) and the precision limit (PL, -x-)

measured per sample over this period for each concentration is normalized to the maximal number of pulses associated with the lowest concentration.

One can observe in figure 13 that the circuit is able to measure DNA concentrations over the whole tested range. However, due to a 11.6 % precision limit conjugated to a small slope of the measurement curve in the low concentrations, the detection limit is of about 0.1 ng/μL.

Nevertheless, for the very low DNA concentrations, a weak number of pulses are expected. It is thus important to increase the measurement time to observe a significant response. Figure 14 shows a 20 seconds measurement for the different concentrations presented above, and of two additional concentrations (i.e. from 400 pg/μL to 40 fg/μL).

On this figure, a non-ambiguous detection appears maintained down to the lowest tested DNA concentration (i.e. 40 fg/μL).

10. Improvements

One of the major limits of the system is the increase of the standard deviation of light measurements for low DNA concentrations. To reduce these variations, a first step could
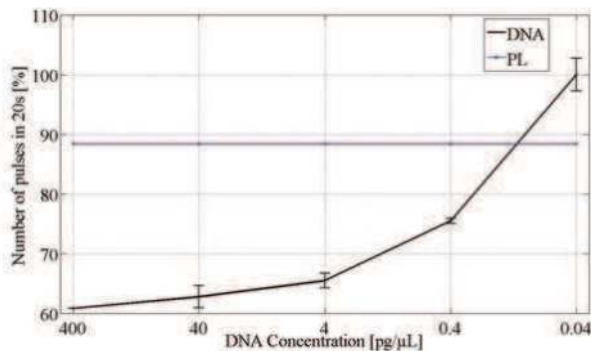

Fig. 14. DNA concentration measurement from 400 pg/μL to 40 fg/μL for 260 nm with the I-f circuit during a 20 seconds measurement period (solid line) and the precision limit (PL, -x-)

be to measure replicates and multiply the number of measurements therefore reducing the standard deviation. On the other hand, the mechanical setup may be improved. With the miniaturization of a future completely portable system, more combined measurements (e.g. concentrations, wavelengths and distances) or increasing the optical dynamic of the system (e.g. by modulating the LED power or improving the photodiode responsivity as demonstrated in Bulteel & Flandre (2009)). Regarding the integrated circuit, a digital system interface (e.g. a digital counter) can be included to automatically take measurements on a definite time period. The interface could send the data to a monitored interface by ZigBee of Wifi modulation as already made with other biological sensors (André et al., 2010). In the future the system may be adapted to measure in the air particles that respond optically to UV light. The DNA container may also be replaced by a microfluidic channel.

11. Conclusion

Our experimentations have proven the ability of new photosensors implemented in SOI technology and combined with UV LEDs to establish a monotonic relation between a DNA concentration and the resulting photocurrent after UV transmittance through assay microtubes containing the samples under test. The photodiode alone achieves a current measurement precision of 2 % and a detection range over 5 decades of concentrations, down to 4 pg/μL in optimal conditions. The threshold of quantification was estimated at 20 pg/μL. With the same PCR tubes, the photodiode is also able to establish a relation between the diode photocurrent and bacteria samples. The integrated circuit including a SOI photodiode and a CMOS current-to-frequency converter is able to measure DNA concentration down to 40 fg/μL with a precision of about 10 %. Compared to optical apparatus and laboratory equipments commonly used to quantify the concentration of biological samples, the detection limits are improved with a very high accuracy. The SOI technology next offers the possibility to integrate the measurement setup into a complete lab-on-a-chip, while the miniaturized components of the system will drive a cost reduction.

12. Acknowledgments

13. References

Afzalian, A.; Flandre, A. (2005) Physical Modeling and Design of Thin-Film SOI Lateral PIN Photodiodes. *IEEE Transactions on Electron Devices*, Vol. 52, No. 6, pp. 1116-1122, June 2005, ISSN 0018-9383

Afzalian, A.; Flandre, D. (2006) Monolithically integrated 10Gbit/s photodiode and transimpedance amplifier in thin-film SOI CMOS technology. *IEE Electronics Letters*, Vol. 42, No. 24, pp. 1420-1421, ISSN 0013-5194

Andre, N.; Druart, S.; Gerard, P.; Pampin, R.; Moreno-Hagelsieb, L.; Kezai, T.; Francis, L.; Flandre, D.; Raskin, J.-P. (2010) Miniaturized Wireless Sensing System for Real-Time Breath Activity Recording. *IEEE Sensors Journal*, Vol.10, Issue 1, pp. 178 - 184, January 2010, ISSN 1530-437X

Biyikli, N.; Kimukin, I.; Tut, T.; Aytur, O.; Ozbay, E. (2005) Fabrication and characterization

of solar-blind $Al_{0.6}Ga_{0.4}N$ MSM photodetectors. *Electronics Letters*, Vol. 41, No. 5, pp. 274-275, March 2005, ISSN 0013-5194

Bolton, E.; Sayler, G.; Nivens, D.; Rochelle, J.; Ripp, S.; Simpson, M. (2001) Integrated CMOS photodetectors and signal processing for very low-level chemical sensing with the bioluminescent bioreporter integrated circuit. *Sensors and actuators. B, Chemical A.*, Bol. 85, No. 1-2, pp. 179-185, June 2002, ISSN 0925-4005

Brown, D.; Downey, E.; Kretchmer, J.; Michon, G.; Shu, E.; Schneider, D. (1998) SiC Flame Sensors for Gas Turbine Control Systems. *Solid-state electronics*, Vol. 42, No. 5, pp. 755-760, ISSN 0038-1101

Bulteel, O.; Dupuis, P.; Jeumont, S.; Irenge, L.; Ambroise, J.; Macq, B.; Gala, J.-L.; Flandre,D. (2009) Low-cost miniaturized UV photosensor for direct measurement of DNA concentration within a closed tube container, *Proceedings of the fourth European congress for medical and biomedical engineering 2008*, pp. 1057-1061, ISBN 978-3-540-89207-6, Springer, Berlin

Bulteel, O.; Afzalian, A.; Flandre, D. (2009) Fully integrated blue/UV SOI CMOS photosensor for biomedical and environmental applications. *Analog Integrated Circuit Signal Processing*, Springer, October 2009, ISSN 1573-1979

Bulteel, O.; Flandre, D. (2009) Optimization of Blue/UV Sensors Using PIN Photodiodes in Thin-Film SOI Technology, *ECS Transactions of 215th ECS Meeting*, Vol. 19, Issue 4, pp. 175-180, San Francisco, CA, May 2009 , Omura, Y.; Cristoloveanu, S.; Gamiz, F.; Nguyen, B.

Chang, S.; Ko, T.; Su, Y.; Chiou, Y.; Chang, C.; Shei, S.; Sheu, J.; Lai, W.; Lin, Y.; Chen, W.; Shen, C. (2006) GaN-Based p-i-n Sensors With ITO Contacts. *IEEE Sensors Journal*, Vol. 6, No. 2, pp. 406-411, April 2006, ISSN 1530-437X

Chang, S.; Fang, Y.; Hsu, K.; Wei, T. (2008) GaN UV MSM photodetector on porous β-SiC/(111)Si substrates. *Sensors and actuators. A, Physical*, Vol. 147, No. 1, pp. 1-5, September 2008, ISSN 0924-4247

Chen, Y.; du Plessis, M. (2006) An integrated 0.35 μm CMOS optical receiver with clock and data recovery circuit. *Microelectronics Journal*, Vol. 37, Issue 9, September 2006, pp. 985-992

Chu, J.; Huang, S.; Zhu, H.; Xu, X.; Sun, Z.; Chen, Y.; Huang, H. (2008) Preparation of indium thin films without external heating for application in solar cells. *Journal of Non-Crystalline Solids*, Vol. 354, Issues 52-54, December 2008, pp. 5480-5484, ISSN 0022-3093

Fang, Y.; Hwang, S.; Chen, K.; Liu, C.; Tsai, M.; Kuo, L. (1992)An Amorphous SiC/Si Heterojunction p-i-n Diode for Low-Noise and High-Senstivity UV Detector. *IEEE Transactions on Electron Devices*, Vol. 39, No. 2, pp. 292-296, February 1992, ISSN 0018-9383

Filanovsky, I.; Baltes, H. (1994) CMOS Schmitt trigger design. *IEEE Transactions on Circuits and Systems*, Vol. 41, Issue 1, January 1994, pp. 46-49, ISSN 1057-7122

Flandre, D.; Colinge, J.-P.; Chen, J.; De Ceuster, D.; Eggermont, J.-P.; Ferreira, L.; Gentinne, B.; Jespers, P.; Viviani, A.; Gillon, R.; Raskin, J.-P.; Vander Vorst, A.; Vanhoenacker-Janvier, D.; Silveira, F. (1999) Fully-Depleted SOI CMOS Technology for Low-Voltage Low-Power Mixed Digital/Analog/Microwave Circuits. *Analog Integrated Circuits and Signal Processing*,Vol. 21, No. 3, Decembre 1999, pp. 213-228, ISSN 0925-1030

Flandre, D.; Adriaensens, S.; Akheyara, A.; Crahay, A.; Demeûs, L.; Delatte, P.; Dessard,

V.; Iniguez, B.; Nève, A.; Katschmarskyj, B.; Loumaye, P.; Laconte, J.; Martinez, I.; Picun, G.; Rauly, E.; Renaux, C.; Spôte, D.; Zitout, M.; Dehan, M.; Parvais, B.; Simon, P.; Vanhoenacker, D.; Raskin, J.-P.(2001) Fully depleted SOI CMOS technology for heterogeneous micropower, high-temperature or RF microsystems. *Solid-State Electronics*, Vol. 45, No. 4, April 2001, pp. 541-549, ISSN 0038-1101

Gombert, A.; Glaubitt, W.; Rose, K.; Dreibholz, J.; Bläsi, B.; Heinzel, A.; Sporn, D.; Döll, W.; Wittwer, V. (2000) Antireflective transparent covers for solar devices. *Solr Energy*, Vol. 68, No. 4, pp. 357-360, 2000, ISSN 0038-092X

Han, K.-S.; Lee, H.; Kim, D.; Lee, H. (2009) Fabrication of anti-reflection structure on protective layer of solar cells by hot-embossing method. *Solar Energy Materials and Solar Cells*, Vol. 93, Issue 8, August 2009, pp. 1214-1217, ISSN 0927-0248

Karczemska, A. & Sokolowska, A. (2001). Materials for DNA sequencing chip, *3rd International Conference on Novel Applications of Wide Bandgap Layers*, pp. 176, 0-7803-7136-4, Zakopane - Poland, June 2001, IEEE, Zakopane

Kumer, B.; Pandian, T.; Seekiran, E.; Narayanan, S. (2005) Benefit of dual layer silicon nitride anti-reflection coating, *Record of the Thirty-first IEEE Photovoltaic Specialists Conference 2005*, pp. 1205-1208, ISSN 0160-837, Pangalore, January 2005, pages 1205-1208, 2005

Luque, A.; Vasquez, D.; Rueda, A. (2003) Leakage current and charge injection measurement in thin-film SOI switches, *XVIII conference on Design of Circuits and Integrated Systems*, pp. 706-710

Miura, N.; Chiba, T.; Yamada, H.; Baba, S. (2007) Development of Silicon-on-Insulator (SOI) Uv Sensor IC, in *OKI Technical Review* ,Vol. 74, No. 3, Issue 221, pp.38-39, October 2007

Monroy, E.; Calle, F.; Pau, J.; Muñoz, E.; Omès, F.; Beaumont, B.; Gibart, P. (2001) AlGaN-based UV photodetectors. *Journal of crystal growth*, Vol. 230, No. 3-4, pp. 537-543, ISSN 0022-0248

Pauchard, A.; Rochas, A.; Randjelovic, Z.; Besse, P; Popovic, R. (2000) Ultraviolet Avalanche Photodiode in CMOS Technology, *Electron Devices Meeting, 2000. IEDM Technical Digest. International*, pp. 709-712, 0-7803-6438-4, San Francisco, December 2000, IEEE, San Francisco

Ripp, J. (1996) Analytical detection limit guidance & Laboratory Guide for Determining Method Detection Limits, *Wisconsin Department of Natural Resources Laboratory Certification Program*, Jeffrey Ripp, Wisconsin Department of Natural Resources, PUBL-TS-056-96, Madison (WI)

Simpson, M.; Sayler, G.; Patterson, G; Nivens, D.; Bolton, E.; Rochelle, J.; Arnott, J.; Applegate, B.; Ripp, S.; Guillorn, M. (2001) An integrated CMOS microluminometer for low-level luminescence sensing in the bioluminescent bioreporter integrated circuit. *Sensors and Actuators, B: Chemical, A.*, Vol. 72, No. 2, pp. 134-140, January 2001, ISSN 0925-4005

Torres-Costa, V.; Martín-Palma, R.; Martínez-Druart, J. (2007) All-silicon color-sensitive photodetectors in the visible. *Materials Science and Engineering : C*, Vol. 27, Issues 5-8 , September 2007, pp. 954-956, ISSN 0928-4931

Yotter, R. & Wilson, D. (2003) A Review of Photodetectors for Sensing Light-Emitting Reporters in Biological Systems. *IEEE Sensors Journal*, Vol. 3, No. 3, June 2003, pp. 288-303, ISSN 1530-437X

Zimmermann, H. (2000). *Integrated Silicon Optoelectronics*, Springer, 3540666621, Berlin.
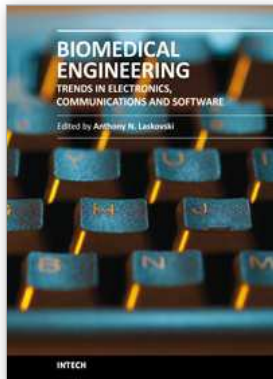
Biomedical Engineering, Trends in Electronics, Communications and Software

Edited by Mr Anthony Laskovski

Rapid technological developments in the last century have brought the field of biomedical engineering into a totally new realm. Breakthroughs in materials science, imaging, electronics and, more recently, the information age have improved our understanding of the human body. As a result, the field of biomedical engineering is thriving, with innovations that aim to improve the quality and reduce the cost of medical care. This book is the first in a series of three that will present recent trends in biomedical engineering, with a particular focus on applications in electronics and communications. More specifically: wireless monitoring, sensors, medical imaging and the management of medical information are covered, among other subjects.

How to reference

In order to correctly reference this scholarly work, feel free to copy and paste the following:

Olivier Bulteel, Nancy Van Overstraeten-Schlögel, Aryan Afzalian, Pascal Dupuis, Sabine Jeumont, Leonid Irenge, Jérôme Ambroise, Benoit Macq, Jean-luc Gala and Denis Flandre (2011). Low-Wavelengths SOI CMOS Photosensors for Biomedical Applications, Biomedical Engineering, Trends in Electronics, Communications and Software, Mr Anthony Laskovski (Ed.), ISBN: 978-953-307-475-7, InTech, Available from: http://www.intechopen.com/books/biomedical-engineering-trends-in-electronics-communications-and-software/low-wavelengths-soi-cmos-photosensors-for-biomedical-applications

INTECH
open science | open minds